The nondetached cells proliferated and only suspension-treated rMSCs became beating cells after 6 weeks of culture (data not shown).

Immunostaining

Immunofluorescence examination clearly showed that when the dishes were stained with anti-troponin T-C antibody, the beating areas were positively stained as shown in Figure 4, but cells treated by monolayer induction remained at the background level of staining.

Expression of cardiomyocyte-associated genes in beating and nonbeating cells

To define the phenotype of the beating cells, the expression levels of cardiac-specific genes *TNNC 1, TNNT 2, TNNC 2, TNNI 3, GATA 4, and MEF2D* were evaluated. Expression levels of given genes were assessed using RNAs from neonatal hearts as positive qualitative controls. The expression levels of *TNNC 1, TNNT 2, and MEF2D* were higher in beating cells than in nonbeating cells, as shown in Figure 5A and B. The expressions of *TNNI 3 and GATA 4* were detected in only one of four isolated colonies of beating cells and were not detected in any nonbeating colonies. The high expression of *TNNC2* in Figure 5A is possibly because either skeletal muscle cells or initial cardiomyocytes are also present in the beating colonies.

In neonatal cardiomyocytes (3 days of cultivation), *TNNC 1, TNNT 2, TNNI 3, and GATA 4* were expressed (Fig. 5A, B). However, *TNNC 2* was not expressed. These data suggested that 25% of the beating cells were cardiomyocytes and 75% were late-maturing cardiomyocytes.

Discussion

MSCs derived from bone marrow are useful cells because they can be isolated from patients and can differentiate into many types of cells. The production of autologous beating cardiomyocytes is an attractive goal for cell-based therapy. However, in previous studies, differentiation into cardiomyocytes occurred at extremely low rates.[7,10] Therefore, it is essential to establish a new, more effective system for differentiating MSCs into beating cardiomyocytes *in vitro* before being transplanted into patients. Other reports have demonstrated that rat and mouse bone marrow cells can differentiate into cardiomyocytes *in vitro*.[10,11] On the other hand, Liu *et al.* reported that 5-azacytidine could not expand rMSCs or induce their differentiation into cardiomyocytes.[12] In our experience from 14 experiments in suspension and monolayer induction, beating cells were obtained in only 7 experiments with suspension induction and in 1 with monolayer induction. These results suggested that beating cardiomyocytes were not easily obtained after exposure to 5-azacytidine. In this regard, the induction method and the substrate are important to obtain beating cardiomyocytes.

Some reports have described manipulating microenvironmental factors, such as cell dimensions, controlled delivery of soluble factors, chemical cues, mechanical cues, and culture substrates, for the controlled differentiation of stem cells.[26,27] Cells in monolayer culture are in a static environment and have a relatively small surface area for diffusion in contrast to cells in suspension culture.[15] In this study, more than 90% of cells induced with suspension method were adhered onto the dishes at 24 h after the cells were inoculated into monolayer cultures (Supplemental Fig. S2 available online at www.liebertonline.com). After 3 weeks in culture, the cells induced by the suspension method were shaped like myotubes on all types of dishes, as shown in Figure 1, and had begun to form colonies. These differentiated myotube shapes were similar to those described by Wakitani *et al.* and Makino *et al.*

In this study, the expression of *TNNT 2* was higher in suspension induction than in monolayer induction, as shown in Figure 2A. On the other hand, *TNNC 1* expression was generally lower in suspension induction than in monolayer induction (Figure 2B). However, the gene expression of *TNNC 2* was detected only with the suspension induction and not with the monolayer induction (Figure 2C). These

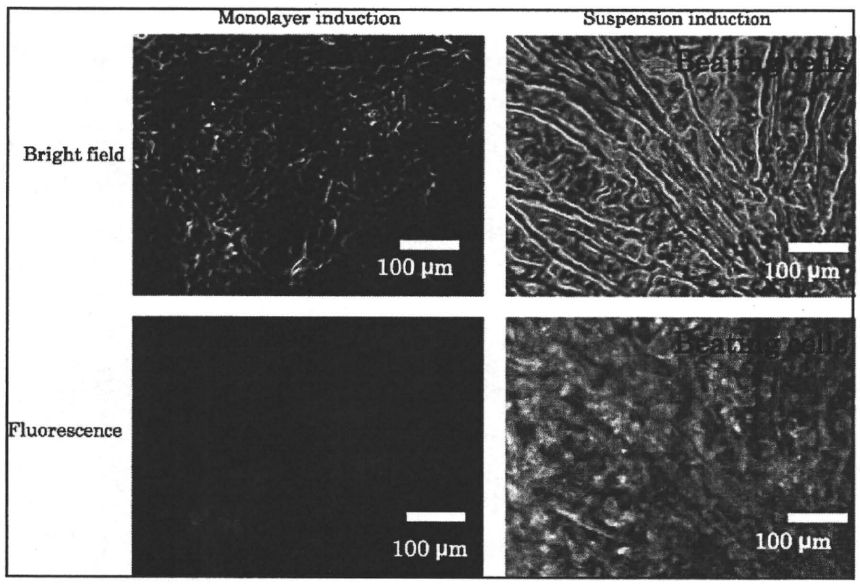

FIG. 4. rMSCs induced by monolayer or suspension method were stained with anti-troponin T-C antibody.

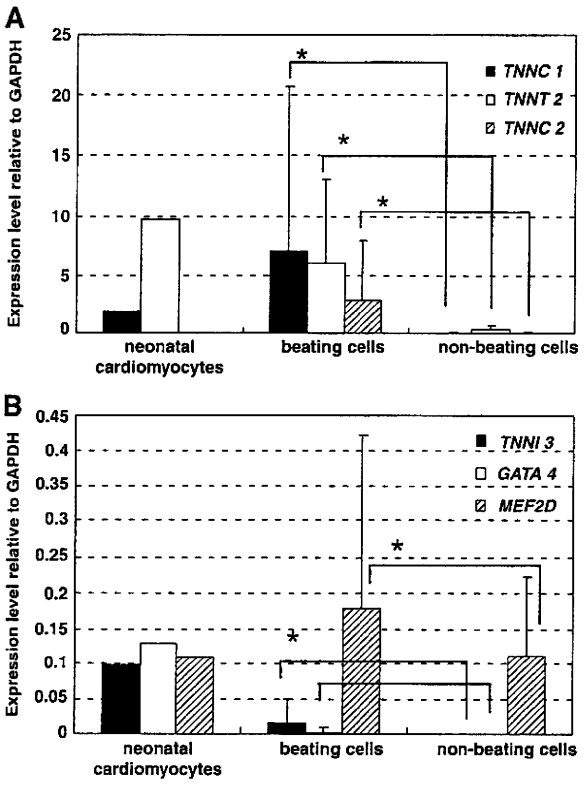

FIG. 5. (A) Expression levels of *TNNC 1*, *TNNT 2*, and *TNNC 2*, (B) *TNNI 3*, *GATA 4*, *and MEF2D* in the four colony types of beating and nonbeating cells after suspension induction. Cardiomyocytes isolated from rat neonatal heart were also evaluated after 3 days of cultivation as a qualitative positive control. Data are means ± standard deviation; $n = 4$ for each sample; $^*p < 0.2$.

results indicated that differentiation efficiency was affected by suspension induction. The enhancement mechanism is unclear but may be related to the proliferation activity, which had not yet started in the suspension condition.

The expression levels of cardiac-specific genes *TNNT 2*, *TNNC 1*, *and MEF2D* of the beating cells were higher than those of nonbeating cells and almost the same level as those of neonatal cardiomyocytes. The beating of neonatal cardiomyocytes weakens with culture time. In these experiments, the gene expression of neonatal cardiomyocytes was measured at 3 days after cultivation, to use the well-beating cardiomyocytes as control cells.

Troponin, a calcium-receptive protein complex involved in the contraction of striated muscles, consists of three components: a calcium-binding component (troponin C), a component that inhibits contractile interaction (troponin I), and a tropomyosin-binding component (troponin T).[28] These contractile proteins are expressed in the developing mammalian heart.[24] Therefore, cardiac troponin T (*TNNT2*), slow troponin C (*TNNC1*), and cardiac troponin I (*TNNI 3*) are known to be markers of cardiomyocytes.[23,24] Myocyte enhancer factor (*MEF2*) genes are recognized to be expressed in differentiated skeletal and cardiac muscle.[29] *MEF2D* and *GATA-4* are regulatory factors for cardiac troponin I.[30] Arceci *et al.* and Edmondson *et al.* reported that the *GATA-4* gene was expressed in the early stage[31] and *MEF2D* in the middle stage of heart development.[32] Fukuda also reported that the *MEF2D* gene was expressed in cardiomyogenic cells after differentiation.[33] Consequently, in this study, we measured the expression of *TNNT2, TNNC1, TNNC2, TNNI3, GATA-4, and MEF2D* to examine the differentiation of rMSCs to cardiomyocytes.

Akavia *et al.* reported that *GATA 4* and *TNNI 3* were expressed only in cardiac muscle cells and not skeletal muscle cells.[34] However, the expression levels were decreased by culture time and were almost undetectable after 10 days of culture for *TNNI 3*. Referring to this report, we successfully differentiated the MSCs into beating cardiomyocytes by suspension induction. We concluded that expression of *GATA 4* and *TNNI 3* was not detected in the other three beating colonies because of the long cultivation period. *TNNC 2* was also expressed in beating cells. The high expression of *TNNC2*, shown in Figure 5A, is possibly because either skeletal muscle cells or initial cardiomyocytes were also present in the beating colonies. As shown in Figure 3, *TNNC 2* expression was decreased by the culture period. This observation was similar to that of Stoutamyer and Dhoot, who detected *TNNC 2* on day 3 in quail hearts *in ovo* but could not detect it by day 17 using RT-PCR.[23]

Interestingly, our results indicated that the spontaneously beating cells were detected only on ECM protein-coated dishes and were induced with suspension induction. The beating cells or colonies were not detected in noncoated polystyrene dishes. These results indicated that the ECM substrate strongly affected cellular differentiation. The number of beating cell colonies on gelatin-coated dishes was much higher than on other substrate-coated dishes. This was similar to the result in our previous study, in which the beat and the beating period of isolated neonatal rat cardiomyocytes on gelatin-coated dishes were stronger and longer than on fibronectin- or collagen-coated dishes or on noncoated polystyrene dishes.[19] This phenomenon may be related to the cell biological activity and the physical properties of the substrate. It has been reported that during cell culture, large amounts of fibronectin are produced, which associates with collagen in a way that promotes fibrillogenesis.[35] It was also reported that fibronectin binds to gelatin more strongly than to collagen.[35,36] Therefore, fibril might be produced at higher levels on gelatin-coated dishes than on fibronectin- or collagen-coated dishes.

A very large difference was observed in the number of beating colonies on gelatin-coated and collagen type I-coated dishes. The dynamic storage modulus of gelatin is higher than that of collagen type I.[37] The high dynamic storage modulus of gelatin, as well as substantial movement and stretching, may have allowed easier contraction of differentiated rMSCs, which might have contributed to the large difference in the number of beating colonies. It was also reported that the elasticity of the substrate affects the differentiation of naive MSCs and mouse myoblast C2C12 cells into myogenic cells.[38,39]

In this study, cardiac gene expression analysis and immunostaining were performed to verify whether the beating cells derived from treated MSCs were cardiomyocytes or not. The beating cells and colonies were detected at 3 weeks after treatment ended and became synchronous after 1 week. Therefore, the immunostaining was done at 4 weeks after

treatment ended. The results of immunofluorescence and cardiac gene expression demonstrated that the beating cells expressed cardiomyocyte-like phenotypes.

Conclusion

In conclusion, this study demonstrated that suspension induction is a promising method for differentiating rMSCs into cardiomyocytes *in vitro*. In addition, the ECM protein is seen to affect the differentiation of rMSCs into beating cells. These findings indicate a bright future for the production of autologous beating cardiomyocytes for cell-based therapy and myocardial patch scaffold. In this study, a gelatin-based niche was found to be preferable for cardiac differentiation and beating function. Nevertheless, further study is required to characterize the full mechanism of the suspension method for the differentiation of MSCs into cardiomyocytes as well as the effect of differentiated MSCs after transplantation *in vivo*.

Acknowledgments

This work was supported by a CREST-JST and partly supported by a Grant-in-Aid for Scientific Research (B) from the Ministry of Education, Culture, Sports, Science, and Technology of Japan. The authors thank Dr. Tomo Ehashi for his outstanding technical assistance. The primary author A. Miskon thanks the Ministry of Higher Education of Malaysia and Tun Hussein Onn University of Malaysia for funding his study under the Academic Training Scheme.

Disclosure Statement

No competing financial interests exist.

References

1. Lopez, A.D., Mathers, C.D., Ezzati, M., Jamison, D.T., and Muray, C.J. Global and regional burden of disease and risk factors, 2001: systematic analysis of population health data. Lancet **367,** 1747, 2006.
2. Rose, E.A., Gelijins, A.C., Moskowitz, A.J., Heitjan, D.F., Stevenson, L.W., Dembitsky, W., Long, J.W., Ascheim, D.D., Tierney, A.R., Levitan, R.G., Watson, J.T., Meier, P., Ronan, N.S., Shapiro, P.A., Lazar, R.M., Miller, L.W., Gupta, L., Frazier, O.H., Desvigne-Nickens, P., Oz, M.C., and Poirer, V.L. Randomized Evaluation of Mechanical Assistance for the Treatment of Congestive Heart Failure (REMATCH) study group. Long-term mechanical left ventricular assistance for the end-stage heart failure. N Engl J Med **345,** 1435, 2001.
3. Bank, A.J., Mir, S.H., Nguyen, D.Q., Bolman, R.M., Shumway, S.J., Miller, L.W., Kaiser, D.R., Ormaza, S.M., and Park, S.J. Effects of left ventricular assist devices on outcomes in patients undergoing heart transplantation. Ann Thorac Surg **69,** 1369, 2000.
4. Lietz, K., and Miller, L.W. Will left-ventricular assist device therapy replace heart transplantation in the foreseeable future? Curr Opin Cardiol **20,** 132, 2005.
5. Miyahara, Y., Nagaya, N., Kataoba, M., Yanagawa, B., Tanaka, K., Hao, H., Ishino, K., Ishida, H., Shimisu, T., Kangawa, K., Sano, S., Okano, T., Kitamura, S., and Mori, H. Monolayered mesenchymal stem cells repair scarred myocardium after myocardial infarction. Nat Med **12,** 459, 2006.
6. Wollert, K.C., and Drexler, H. Clinical applications of stem cells for the heart. Circ Res **96,** 151, 2005.
7. Arnado, L.C., Saliaris, A.P., Schuleri, K.H., St. John, M., Xie, J.S., Cattaneo, S., Durand, D.J., Fitton, T., Kuang, J.Q., Stewart, G., Lehrke, S., Baumgartner, W.W., Martin, B.J., Heldman, A.W., and Hare, J.M. Cardiac repair with intramyocardial injection of allogenic mesenchymal stem cells after myocardial infarction. Proc Natl Acad Sci USA **102,** 11474, 2005.
8. Jackson, K.A., Majka, S.M., Wang, H., Pocius, J., Hartley, C.J., Majesky, M.W., Entman, M.L., Michael, L.H., Hirschi, K.K., and Goodell, M.A. Regeneration of ischemic cardiac muscle and vascular endothelium by adult stem cells. J Clin Invest **107,** 1395, 2001.
9. Oakley, R.M.E., Ooi, C.O., Bongso, A., and Yacoub, M.H. Myocyte transplantation for myocardial repair: a few good cells can mend a broken heart. Ann Thorac Surg **71,** 1724, 2001.
10. Wakitani, S., Saito, T., and Caplan, A.I. Myogenic cells derived from rat bone marrow mesenchymal stem cells exposed to 5-azacytidine. Muscle Nerve **18,** 1417, 1995.
11. Makino, S., Fukuda, K., Miyoshi, S., Konishi, F., Kodama, H., Pan, J., Sano, M., Takahashi, T., Hori, S., Abe, H., Hata, J., Umezawa, A., and Ogawa, S. Cardiomyocytes can be generated from marrow stromal cells *in vitro*. J Clin Invest **103,** 697, 1999.
12. Liu, Y., Song, J., Liu, W., Wan, Y., Chen, X., and Hu, C. Growth and differentiation of rat bone marrow stromal cells: does 5-azacytidine trigger their cardiomyogenic differentiation? Cardiovasc Res **58,** 460, 2003.
13. Xu, W., Zhang, X., Qian, H., Zhu, W., Sun, X., Hu, J., Zhou, H., and Chen, Y. Mesenchymal stem cell from adult human bone marrow differentiate into a cardiomyocyte phenotype *in vitro*. Exp Biol Med (Maywood) **229,** 623, 2004.
14. Clemmons, D.R., Elgin, R.G., Han, V.K., Casella, S.J., D'Ercole, A.J., and Van Wyk, J.J. Cultured fibroblast monolayers secrete a protein that alters the cellular binding of somatomedin-C/insulin-like growth factor I. J Clin Invest **77,** 1548, 1986.
15. Griffin, S.J., and Houston, J.B. Prediction of *in vitro* intrinsic clearance from hepatocytes: comparison of suspensions and monolayer cultures. Drug Metab Dispos **33,** 115, 2005.
16. Groothuis, G.M., and Meijer, D.K. Drug traffic in the hepatobiliary system. J Hepatol **24 Suppl 1,** 3, 1996.
17. Langer, R., and Vacanti, J.P. Tissue engineering. Science **260,** 920, 1993.
18. Boudreau, N.J., and Jones, P.L. Extracellular matrix and integrin signalling: the shape of things to come. Biochem J **339,** 481, 1999.
19. Miskon, A., Ehashi, T., Mahara, A., Uyama, H., and Yamaoka, T. Beating behavior of primary neonatal cardiomyocytes and cardiac-differentiated P19.CL6 cells on different extracellular matrix components. J Artif Organs **12,** 111, 2009.
20. Huang, N.F., Lee, R.J., and Li, S. Chemical and physical regulation of stem cells and progenitor cells: potential for cardiovascular tissue engineering. Tissue Eng **13,** 1809, 2007.
21. Seglen, P.O. Preparation of isolated rat liver cells. Methods Cell Biol **13,** 29, 1976.
22. Moldeus, P., Hogberg, J., and Orrenius, S. Isolation and use of liver cells. Methods Enzymol **52,** 60, 1978.
23. Stoutamyer, A., and Dhoot, G.K. Transient expression of fast troponin C transcripts in embryonic quail heart. J Muscle Res Cell Motil **26,** 237, 2005.

24. Saggin, L., Ausoni, S., Gorza, L., Sartore, S., and Schiaffino, S. Troponin T switching in the developing rat heart. J Biol Chem **263,** 18488, 1998.
25. Taylor, S.M., and Jones, P.A. Multiple new phenotypes induced in 10T1/2 and 3T3 cells treated with 5-azacytidine. Cell **17,** 771, 1979.
26. Hwang, N.S., Varghese, S., and Elisseeff, J. Controlled differentiation of stem cells. Adv Drug Deliv Rev **60,** 199, 2008.
27. Burdick, J.A., and Vunjak-Novakovic, G. Review: engineered microenvironments for controlled stem cell differentiation. Tissue Eng Part A **15,** 205, 2009.
28. Ebashi, S. Regulatory mechanism of muscle contraction with special reference to the Ca-troponin-tropomyosin system. Essays Biochem **10,** 1, 1974.
29. Yu, Y.T., Breitbart, R.E., Smoot, L.B., Lee, Y., Mahdavi, V., and Nadal-Ginard, B. Human myocyte-specific enhancer factor 2 comprises a group of tissue-restricted MADS box transcription factors. Genes Dev **6,** 1783, 1992.
30. Di Lisi, R., Millino, C., Calabria, E., Altruda, F., Schiaffino, S., and Ausoni, S. Combinatorial cis-acting elements control tissue-specific activation of the cardiac troponin I gene *in vitro* and *in vivo*. J Biol Chem **273,** 25371, 1998.
31. Arceci, R.J., King, A.A., Simon, M.C., Orkin, S.H., and Wilson, D.B. Mouse GATA-4: a retinoic acid-inducible GATA-binding transcription factor expressed in endodermally derived tissues and heart. Mol Cell Biol **13,** 2235, 1993.
32. Edmondson, D.G., Lyons, G.E., Martin, J.F., and Olson, E.N. Mef2 gene expression marks the cardiac and skeletal muscle lineages during mouse embryogenesis. Development **120,** 1251, 1994.
33. Fukuda, K. Molecular characterization of regenerated cardiomyocytes derived from adult mesenchymal stem cells. Congenital Anom **42,** 1, 2002.
34. Akavia, U.D., Veinblat, O., and Benayahu, D. Comparing the transcriptional profile of mesenchymal cells to cardiac and skeletal muscle cells. J Cell Physiol **216,** 663, 2008.
35. Dzamba, B.J., Wu, H., Jaenisch, R., and Peters, D.M. Fibronectin binding site in type I collagen regulates fibronectin fibril formation. J Cell Biol **121,** 1165, 1993.
36. Engvall, E., Ruoslahti, E., and Miller, E.D. Affinity of fibronectin to collagens of different genetic types and to fibrinogen. J Exp Med **147,** 1584, 1978.
37. James, C.W.C., and Chang, E.P. Dynamic mechanical and rheo-optical studies of collagen and gelatin. Biopolymers **11,** 2015, 1972.
38. Engler, A.J., Griffin, M.A., Sen, S., Bönnemann, C.G., Sweeney, H.L., and Discher, D.E. Myotubes differentiate optimally on substrates with tissue-like stiffness: pathological implications for soft or stiff microenvironments. J Cell Biol **166,** 877, 2004.
39. Engler, A.J., Sen, S., Sweeney, H.L., and Discher, D.E. Matrix elasticity directs stem cell lineage specification. Cell **126,** 677, 2006.

Address correspondence to:
Tetsuji Yamaoka, Ph.D.
Department of Biomedical Engineering
Advanced Medical Engineering Center
National Cardiovascular Center Research Institute
5-7-1 Fujishirodai
Suita
Osaka 565-8565
Japan

E-mail: yamtet@ri.ncvc.go.jp

Received: April 2, 2009
Accepted: December 14, 2009
Online Publication Date: January 25, 2010

Biomaterials 31 (2010) 4231–4237

Contents lists available at ScienceDirect

Biomaterials

journal homepage: www.elsevier.com/locate/biomaterials

Continuous separation of cells of high osteoblastic differentiation potential from mesenchymal stem cells on an antibody-immobilized column

Atsushi Mahara [1], Tetsuji Yamaoka*

Department of Biomedical Engineering, Advanced Medical Engineering Center, National Cardiovascular Center Research Institute, Suita, Japan

Biomaterials 31 (2010) 4231–4237

Contents lists available at ScienceDirect

Biomaterials

journal homepage: www.elsevier.com/locate/biomaterials

Continuous separation of cells of high osteoblastic differentiation potential from mesenchymal stem cells on an antibody-immobilized column

Atsushi Mahara [1], Tetsuji Yamaoka*

Department of Biomedical Engineering, Advanced Medical Engineering Center, National Cardiovascular Center Research Institute, Suita, Japan

ARTICLE INFO

Article history:
Received 24 December 2009
Accepted 21 January 2010
Available online 24 February 2010

Keywords:
Mesenchymal stem cells
Selection
Interface
Osteoblast

ABSTRACT

Here, we report that two distinctive cell populations with osteoblastic differentiation ability were found in adherent cell populations from bone marrow. Mesenchymal stem cells (MSCs) were conventionally isolated by using adherent property of bone marrow cells onto a plastic culture dish. MSCs enriched on the basis of their adherent property were considered phenotypically and functionally heterogeneous. We developed a ligand-immobilized surface for separating subpopulation of adherent cells derived from bone marrow by the cell rolling process. We successfully isolate two cell populations with high differentiation ability for osteoblasts in adherent bone marrow cells by using the anti-CD34 antibody-immobilized column. The antibody was covalently conjugated with polyacrylic acid and introduced onto the inner surface of a silicone tube. When cell suspension of MSCs was injected into the antibody-immobilized column, different cell populations were isolated. After the cultivation of isolated cells in the osteoblastic differentiation medium for 1 week, few sub-populations were strongly induced to form osteoblastic cells. This study revealed that the ligand-immobilized surface can be used to continually separate cell populations under a labeling-free condition.

1. Introduction

It is widely known that adherent cells found in bone marrow have an ability to differentiate into osteoblasts, adipocytes and chondrocytes. That stem cell is generally named as marrow stromal cells or mesenchymal stem cells (MSCs). Cell differentiation property and its mechanisms have been widely studied in clinical and biological fields. In particular, the field of regenerative medicine focuses on tissue derived stem cells for autologous cell transplantation [1,2]. One important finding is that MSCs, which exist in not only bone marrow but also cord blood and adipose tissue, have therapeutic potential for heart, neural, and brain diseases [3–5]. A standard procedure for isolation of MSCs was reported by Pittenger et al. [6]. MSCs are easily separated by using the adherent property of bone marrow cells onto plastic culture dishes. Ficoll-Hypaque density gradient centrifugation is also used for separating mononuclear cells containing MSCs [7,8]. Other isolation methods based on selection of non-adherent cell population [9], STRO-1 antibody-recognized antigen level [10], and size-sieved cell population [11] have been reported. Isolation methods based on various combinations of cell surface markers have been reported by many groups [12–16].

Although the adherent property of MSCs has been widely used for their isolation, MSCs enriched on the basis of their adherent property are considered as phenotypically and functionally heterogeneous [17]. Surface marker characteristics such as marker density and its variation change with the differentiation process and development of MSCs. Surface marker profile of murine MSCs significantly differ with the passage levels [18,19]. CD34 expression of hematopoietic stem cells continuously decreases with the developmental stage [20]. Consequently, the development of a new approach to isolate MSCs population is important for homogeneous separation.

We have recently developed an antibody-immobilized column which can separate CD34-positive KG-1a cells from CD34 negative HL60 cell [21]. The separation mechanism seems to be based on dynamic interaction between cell surface marker (CD34) and immobilized antibody, known as the cell rolling. In nature, cell rolling is mainly observed in blood vessels as an inflammatory response of leukocytes [22], and its mechanism is derived from temporary interaction between cell surface and ligands. Rolling velocity is regulated by the ligand or cell surface receptor density [23–27]. Thus, cells with different rolling velocities are separated on the surface constantly modified with the ligand against a specific cell surface marker. This separation technique would

* Corresponding author. Tel.: +81 6 6833 5012x2637; fax: +81 6 6835 5476.
E-mail addresses: mahara@ri.ncvc.go.jp (A. Mahara), yamtet@ri.ncvc.go.jp (T. Yamaoka).
[1] Tel.: +81 6 6833 5012x2621; fax: +81 6 6835 5476.

0142-9612/$ – see front matter © 2010 Elsevier Ltd. All rights reserved.
doi:10.1016/j.biomaterials.2010.01.126

principally enable a labeling-free process, and the isolated cells are not contaminated with fluorescent or magnetic-labeled antibody. This procedure would be effective in separating sub-populations of MSCs with different density of surface marker.

In the present study, we applied the antibody-immobilized column to heterogeneous which acquired from murine bone marrow by conventional isolation procedures, and successfully found two different populations in the crude MSCs. The fractions of MSCs were cultured under an osteoblastic differentiation condition for 1 week, and gene expression of specific markers was analyzed by real-time polymerase chain reaction (PCR). To evaluate calcium deposition on the cells, staining with alizarine red S solution was carried out.

2. Materials and methods

2.1. Isolation and culture of mouse MSCs

MSCs were collected according to a protocol modified from Tropel et al. [16]. Mouse bone marrow cells (BMCs) were isolated by flushing the marrow cavities of 8–10-weeks-old C57Bl/6 mice (Japan SLC, Inc., Shizuoka, Japan). BMCs were cultured on a polystyrene cell culture dish (Iwaki Glass, Chiba, Japan) with alpha-MEM (Gibco-Invitrogen, Carlsbad, CA) containing 15% fetal bovine serum (FBS; MB Biomedicals, Inc., Eschwege, Germany), 25 U/ml penicillin, and 25 μg/ml streptomycin (Wako Pure Chemical Industries, Ltd., Osaka, Japan). Non-adherent cells were removed by replacing the culture medium after 3 days. The cells were grown to confluency, washed with the medium, and subcultured by using the Trypsin/EDTA kit (Lonza, Walkersville, MD). Confluent cells were plated at 1:2 to 1:3 dilutions. The adherent cells enriched into plastic culture dish with early passage (passage 3 or 4) were subjected to all experiment as crude MSCs.

2.2. Surface marker analysis and cell sorting by fluorescence activated cell sorting

To evaluate the expression of surface markers by fluorescence-activated cell sorting (FACS), cells were suspended in PBS buffer for 30 min at 4 °C with fluorescein- or phenylephrine-conjugated antibodies against the surface markers CD29, CD31, CD34, CD44, CD45, CD81, CD11b and Sca-1. Antibody labeling was performed using the standard protocol. CD29 and CD31 antibodies were purchased from AbD Serotec (Oxford, UK) and Immunotech (Marseille, France), respectively. CD34, CD11b and Sca-1 antibodies were purchased from eBiocience (San Diego, CA). CD44, CD45 and CD81 antibodies were purchased from Pharmingen (San Diego, CA). After labeling with antibodies, 10^4 cells were analyzed with a FACScalibur flow cytometer (BD Biosciences, San Jose, CA). Conventional sorting of cells with different CD34 expression levels was conducted by FACSAria (BD Biosciences), as control experiment.

2.3. Preparation of the anti-CD34 antibody-immobilized column

Silicone tubes with 0.5 mm inner diameter were used as a substrate for the antibody-immobilized column. Graft polymerization of acrylic acid onto the silicone tube surface was conducted as follows. The tube was treated with ozone gas (ON-3-2, Nippon Ozone Co., LTD., Tokyo, Japan) for 4 h, dipped in 10% acrylic acid/methanol solution, and incubated at 60 °C. After 4 h, the tube was washed with water [28,29]. Graft polymerization was confirmed by toluidine blue staining. To immobilize anti-CD34 antibody on the tube surface, the poly(-acrylic acid)-grafted tube was pre-activated with 1-ethyl-3-(3-dimethylaminopropyl) carbodiimide hydrochloride (WSC), filled with the anti-mouse CD34 rat IgG antibody (AbD Serotec) solution at concentration of 10 μg/ml, and incubated at 37 °C for 15 h. The tube was washed with PBS, treated with 1 mM 2-aminoethanol solution for 1 h, and preserved at 4 °C until experimental use. The column length was 10 cm, and the tilt angle was 20°.

2.4. Separation of crude MSCs on the antibody-immobilized column

A total of 2×10^4 cells of crude MSCs in 10 μL PBS were injected into the column. The column was flushed with PBS buffer at the flow rate of 50 μL/min until the flow

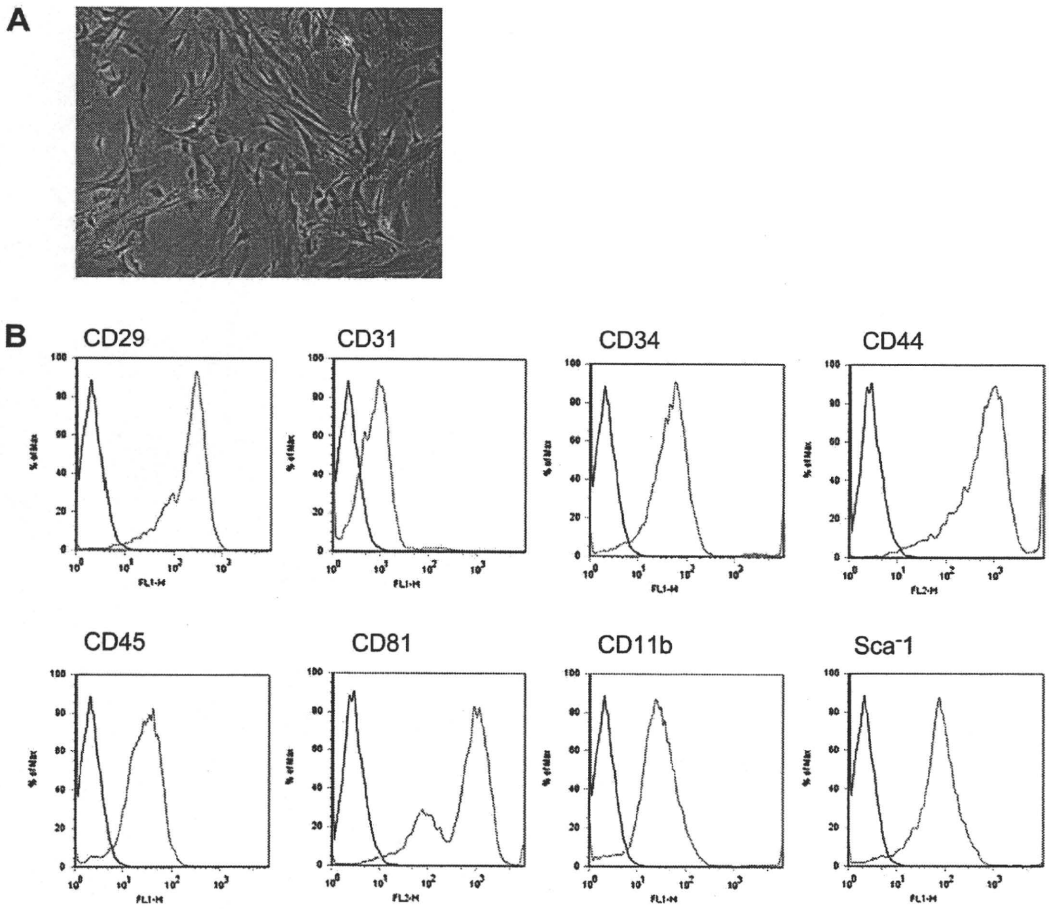

Fig. 1. (A) Morphology of murine MSCs culture. Cultured cells contained some type of cells like small round cells and fibroblast-like cells. (B) Surface marker expression of murine MSCs at passage 2. MSCs were stained with an FITC or PE-labeled antibody. Staining cells were shown in red histogram, and the black is unstained cells as control. These data were confirmed by 3 independent experiments.

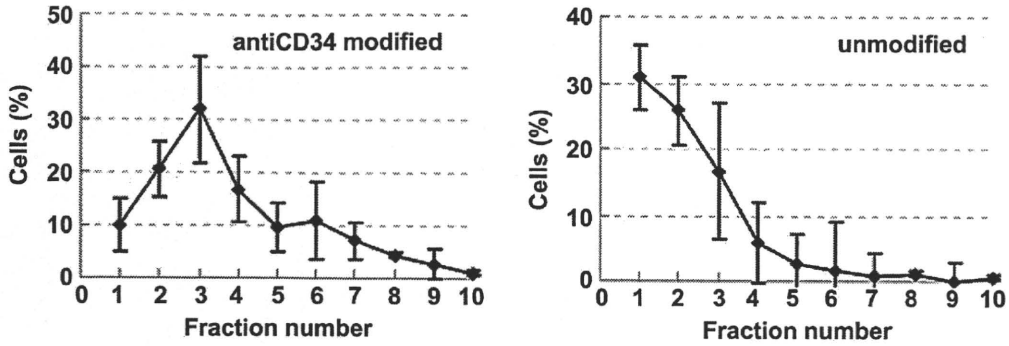

Fig. 2. Elution profiles of murine MSCs on the anti-CD34 antibody-immobilized column or unmodified column. Cell number ratio normalized by the total cell number was plotted against the fraction number. Each data point represents results from 3 independent experiment and the data are presented as mean ± standard error of the means.

volume of 250 μL, and at 600 μL/min thereafter. Eluted cell suspension was collected from top of the column, and cell suspensions were fractionated by elution volume (12.5 μL per fraction). Number and surface marker profile of cells in each fraction was analyzed by the FACS system.

2.5. Differentiation of isolated MSCs into osteoblasts

Purified MSC fractions were acquired from 2×10^4 crude MSCs. MSCs separated on the antibody-immobilized column were cultured on fibronectin-coated 24-well plates (FALCON, Oxnard, CA) with the osteoblastic differentiation medium containing 10^{-8} M dexamethasone, 10 mM β-glycerophosphate, and 0.3 mM ascorbic acid (all three reagents from Sigma–Aldrich, St. Louis, MO). The medium was changed 3 times per week. The cells were fixed with 10% formalin for 20 min at room temperature (RT) and stained with alizarin red S solution.

2.6. Gene expression analysis by real-time PCR

After culturing in differentiation medium for 1 week, total cellular RNA was isolated using Quickgene Mini80 with Quickgene RNA cultured cell kit S (FUJIFILM, Tokyo, Japan). Reverse transcription (ReverTra Ace, TOYOBO Co., LTD., Osaka, Japan) using oligo dT_{18} primer was performed on aliquots (200 ng) of total RNA as a template. The resultant cDNA was used for PCR amplification, and PCR analysis was

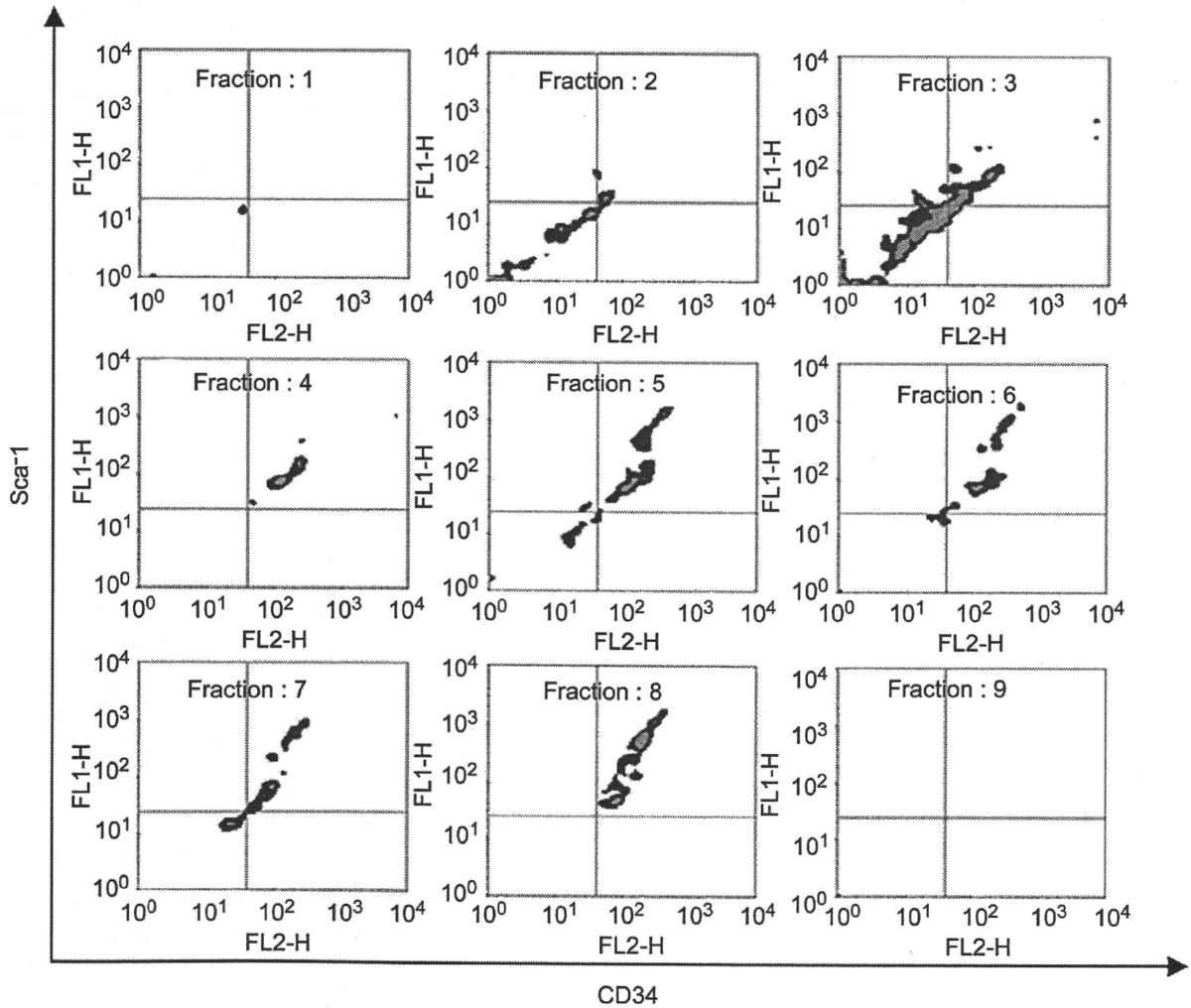

Fig. 3. Surface maker expression of isolated MSCs. Two-dimensional expression analysis of CD34 or Sca-1 was carried out in isolated cells fractions.

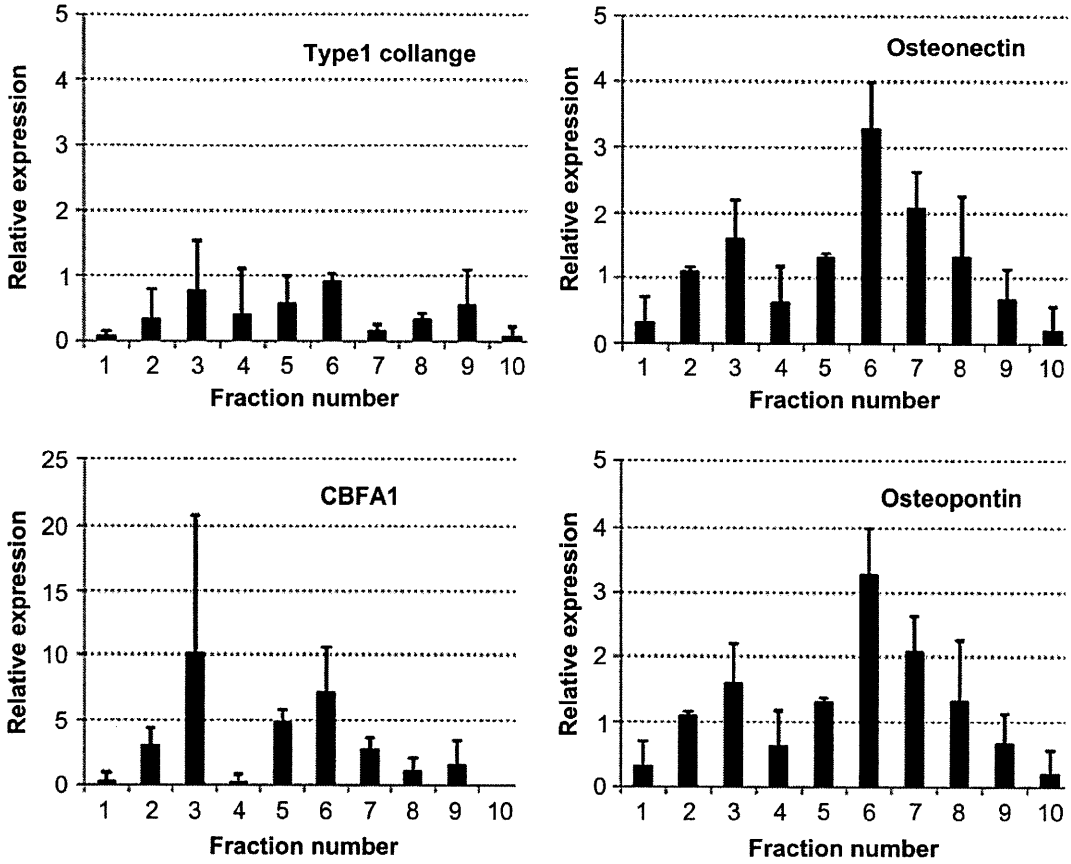

Fig. 4. Gene expression analyses of isolated MSCs on the anti-CD34 antibody-immobilized column for osteoblastic differentiation after 1 week. Relative expression is normalized by the expression of crude MSCs. GAPDH expression level was used as the internal standard control. Each data point represents results from 3 independent experiment and the data are presented as mean ± standard error of the means.

carried out by the GeneAmp 5700 Sequence Detection System (Applied Biosystems, Foster City, CA). PCR primers were designed by Primer Express software (Applied Biosystems). Type 1 collagen, CBFA1, osteopontin and osteonectin were selected as specific marker genes for differentiation. PCR reaction mixture contained 0.52 μL cDNA, 5 pmol of each primer, 25 μL SYBR Green Real-time PCR Master Mix (TOYOBO Co., LTD., Osaka, Japan). Amplification conditions were as follows: 40 cycles of 95 °C for 1 min; 60 °C for 15 s; 74 °C for 1 min. Primers used were (5′ to 3′) CBFA1: CCGCACGACAACCGCACCAT (forward), CGCTCCGGCCCACAAATCTC (reverse); Type 1 collagen: GAAGTCAGCTGCATACAC (forward), AGGAAGTCCAGGCTGTCC (reverse); Osteopontin: TCACCATTCGGATGAGTCTG (forward), ACTTGTGGCTCTGATGTTCC (reverse); Osteonectin: AGCGCCTGGAGGCTGGAGAC (forward), CTTGATGCCAAAG-CAGCCGG (reverse); GAPDH: CAAAATGGTGAAGGTCGGTGTG (forward), ATTT-GATGTTAGTGGGGTCTCG (reverse).

3. Results and discussion

3.1. Surface marker analysis of adherent cell population

MSCs are isolated by the bases of adherent property of bone marrow in some species, such as human [6] and rat [30]. However, it is difficult to isolate homogeneous MSCs by adhesion separation because of unwanted contamination. The crude MSCs displayed a fibroblast-like morphology shown in Fig. 1(A). To eliminate the monocytic cell fraction in adhesion cell population, magnetic beads conjugated with anti-CD11b or anti-CD45 antibodies were used for negative selection [14,16]. Although some surface markers for MSCs were reported in a recent study, homogeneous MSCs could not be identified by such kinds of markers [17,31]. Surface marker expression level of adherent population of murine MSCs are shown in Fig. 1(B). A strong expression of the surface markers CD29, CD44, CD81, and Sca-1, and a weak expression of the surface markers CD34, CD45, and CD11b were observed. No expression of CD31 was observed. Some studies have reported that murine MSCs were positive for the surface markers CD29, CD44 and Sca-1 [14,15,32], and this finding was confirmed in our experimental data. Sca-1 expression level changed with the culture period (data not shown). This phenomenon was already reported in other studies [32]. The MSCs showed a weak and broad expression of CD34, a hematopoietic lineage marker. Umezawa et al. reported that murine MSCs with a low expression of CD34 have a high potential for the regenerative effect in cardiopulmonary disease. CD34 is the progenitor or stem cell marker, and the expression continuously decreased with the culture period. That is, the CD34 expression would be closely related with the differentiation stage. Hence, we chose the anti-CD34 antibody as the immobilized ligand and evaluated the differentiation ability of MSCs isolated on the anti-CD34 antibody-immobilized column.

3.2. Separation profile of MSCs on the anti-CD34 antibody-immobilized column

We have developed a separation column in previous work [21]. Details about the separation column were shown in Materials and methods. The antibody-immobilized column was connected with an injection tube. The length of the column and injection tube was 100 mm. Medium flow into the column was accomplished with a syringe pump. Elution profile of crude MSCs on the anti-CD34 antibody-immobilized column was evaluated by counting the number of eluted cells in each fraction. When the crude MSCs were injected into an unmodified column, almost all the cells were eluted in early fractions. On the other hand, when the crude MSCs were injected into the anti-CD34 antibody-immobilized column,

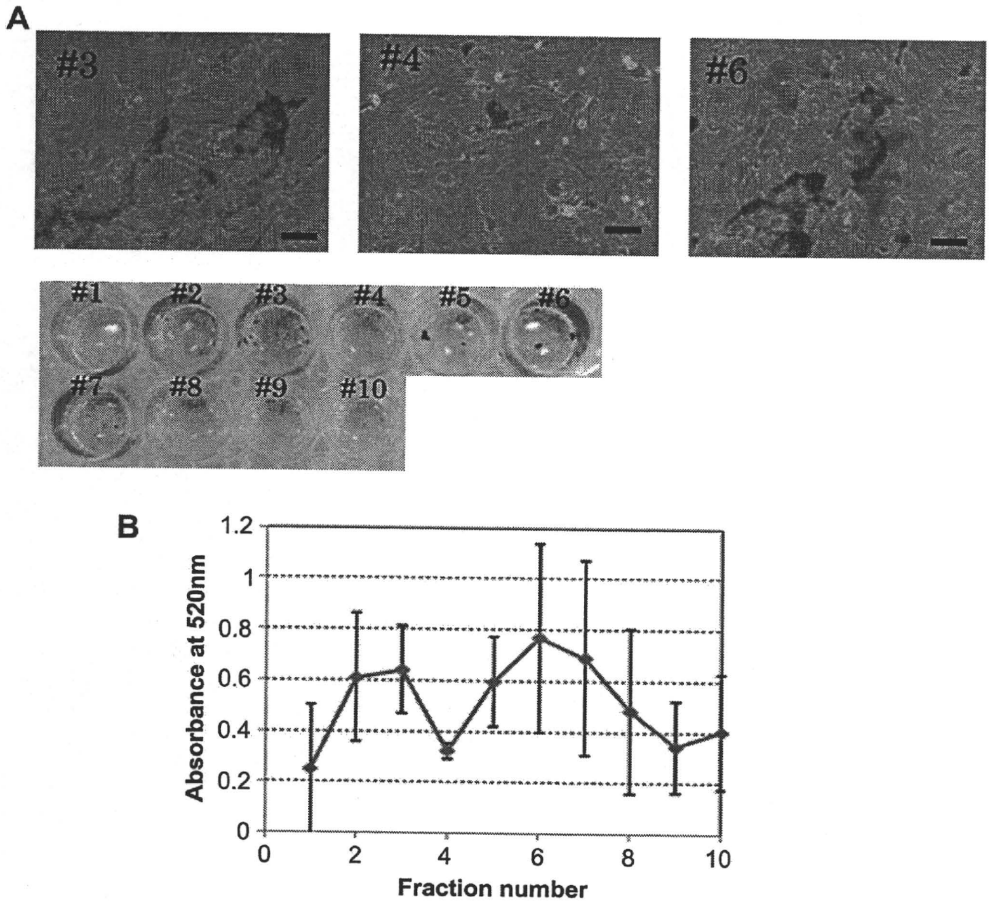

Fig. 5. (A) Photograph of alizarin red S staining MSCs after differentiation for 1 week. Cells were cultured on fibronectin-coated 24-well plate. (B) Quantification of alizarin red S staining in each fraction by absorbance spectrum. Absorption at 540 nm was plotted against the fraction number. Each data point represents results from 3 independent experiment and the data are presented as mean ± standard error of the means.

two peaks were observed (Fig. 2). That is, the delay of cell elution observed in the case of the anti-CD34 antibody-immobilized column probably resulted from the continuous interaction between the surface marker and the immobilized antibody. In our previous work, KG-1a (CD34+) and HL60 (CD34-) cells know as cell line were separated on antibody-immobilized column [21]. In the results, cells were separated by a marker specific manner, and the elution pattern was distinctly depended on the marker expression level. In the case of MSC separation, elution patterns were comparatively broad because of heterogeneity of crude MSCs. Then, surface marker expression of the isolated MSCs on the anti-CD34 antibody-immobilized column was evaluated by FACS. Two-dimensional FACS analysis of CD34 expression against Sca-1 expression is shown in Fig. 3. MSCs with a high expression of CD34 and Sca-1 were presented in later fractions, and a continuous change in the marker expression level was observed with increasing fraction number. These data indicated that the crude MSCs were separated on the column on the basis of the surface marker density. From the above results, we suggest that the antibody-immobilized column could be used to isolate murine MSCs on the basis of their surface marker density.

3.3. *Differentiation of isolated MSCs on the anti-CD34 antibody-immobilized column*

Osteoblastic differentiation was evaluated by gene expression analysis and alizarin red S staining. Type 1 collagen, osteonectin, CBFA1, and osteopontin were selected as specific markers for osteoblastic differentiation. The gene expression level was analyzed in separated MSCs obtained from the column. Type 1 collagen and osteonectin are constantly expressed during osteoblastic differentiation [33–35], while CBFA1 is expressed during the process of maturation. CBFA1 is a transcriptional factor, and the osteopontin expression was promoted by the CBFA1. Fig. 4 shows the expression levels of specific marker genes analyzed by real-time PCR. Type 1 collagen was expressed in almost all fractions, and the expression level was the same as that of crude MSCs. In the case of CBFA1, the expression level in fractions 3, 5, and 6 was higher than that in other fractions. This tendency was the same as that observed for the expression pattern of osteopontin.

CBFA1 is a key factor for mature osteoblastic differentiation. The suppression of CBFA1 expression by mutation of CBFA1 completely restricted bone formation of murine neonatal or newborn [33]. That is, the expression of CBFA1 is necessary for calcium deposition on the cells. The isolated MSCs after differentiation were stained with alizarin red S solution. Fig. 5 shows the picture of stained cells. Isolated MSCs in early fractions (fractions #2- and #3) or later fraction (fractions #5–7) were strongly positive. This staining pattern in terms of the fraction number was similar to that of CBFA1 expression pattern.

These results suggest that separated MSCs in early fraction or later fraction had a high potential for osteoblastic differentiation. It has been reported that osteoblastic progenitor cells were enriched in the CD34-positive population from bone marrow [36]. That is, the cells with high expression of CD34 in later fractions are mainly osteoblastic progenitor cells. It is difficult to determine the origin of these progenitor cells. However, there are two possibilities with

regard to their origin. First, the osteoblastic progenitor cells in bone marrow were contaminated in TCPS-adherent cells. Second, a fraction of MSCs differentiated into progenitor cells during cultivation. Stem cells are difficult to be cultured on a TCPS dish keeping with differentiation properties. Because the environment of MSCs on a culture dish is largely different from that *in vivo*, cultured MSCs have heterogeneous characteristics in terms of surface marker [17] and differentiation property. The purification process of stem cells is important for experimental or clinical use. From these results, we suggested that the ligand-immobilized column could be used to isolate MSCs from the heterogeneous cell populations consisting of progenitor or differentiated cells.

3.4. Differentiation of sorted MSCs by FACS

To verify the effect of surface marker density on the differentiation ability of MSCs, crude MSCs were sorted by FACS as a conventional method for cell separation. Four cell populations were sorted for the evaluation of osteoblastic differentiation (Fig. 6). The CD34 expression level in each population was different, and MSCs with a high density of CD34 were contained in $CD34^{High}FSC^{Low}$ population. In contrast, the low density of CD34 was collected in $CD34^{Low}FSC^{High}$ population. The surface marker density of the cells in $CD34^{High}FSC^{High}$ or $CD34^{Low}FSC^{Low}$ population was almost the same. Fig. 6(B) shows the relative expression of specific marker genes for osteoblastic differentiation. In case of MSCs sorted by FACS, cell population with high and low marker density of CD34 has shown high expression of differentiation markers. This tendency was the same as that observed for separated MSCs on the antibody-immobilized column. This result supported that the two cell populations with high ability for osteoblastic differentiation were present in crude MSCs, and the populations were separated using a CD34 antibody-immobilized column.

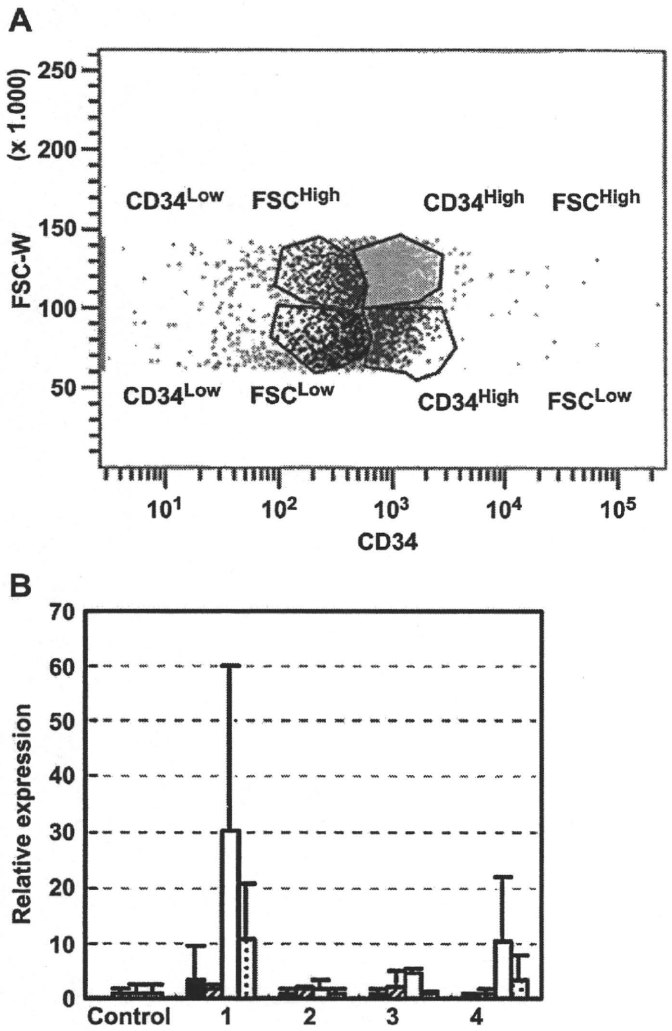

Fig. 6. (A) Sorting regions of isolated cell populations with distinct expression density. Crude MSC populations were divided into four cell populations. Cells with highest CD34 expression density were in the $CD34^{High}FSC^{Low}$ population. On the other hand, cells with lowest expression density were in the $CD34^{Low}FSC^{Hihg}$ population. (B) Gene expression analysis of sorted MSCs by FACS. Sorted MSCs were cultured in the osteoblastic differentiation medium for 8 days. Specific surface markers (bar with lines: type 1 collagen, bar with dots; osteonectin, closed bar; CBFA1, open bar; osteopontin) were analyzed by real-time PCR. Relative expression was normalized by GAPDH. Each data point represents results from 3 independent experiment and the data are presented as mean ± standard error of the means.

4. Conclusion

An anti-CD34 antibody-immobilized column was developed for separating MSCs based on their surface marker density. We selected the anti-CD34 antibody as the immobilized ligand, and crude MSCs were separated on this column. Two cell populations with a high ability for osteoblastic differentiation were purified on this column. MSCs express some surface markers, and their combinations have been explored in many groups in order to specify homogeneous MSCs population. In our approach, marker density is considered as the essential factor for the characterizing MSCs. Two different cell populations could be separated on this column based on their surface marker density. To characterize the cells with a high differentiation ability, it might be effective to use some kinds of ligand-immobilized columns. Further studies on the design of ligand-immobilized surface and construction of the column system are required for effective separation of MSCs.

Acknowledgment

This work was supported by the Research Grant for Cardiovascular Disease (18A-2) from the ministry of Health, Labour and Welfare & Grant-in-Aid for Scientific Research on Innovation Areas (20106014).

Appendix

Figures with essential colour discrimination. Most of the figures (Figs. 1, 3, 5 and 6) in this article have parts that may be difficult to interpret in black and white. The full colour images can be found in the on-line version, at doi:10.1016/j.biomaterials.2010.01.126.

References

[1] Langer R, Vacanti JP. Tissue engineering. Science 1993;260:920–6.
[2] Holden C, Vogel G. Plasticity: time for a reappraisal. Science 2002;296:2126–9.
[3] Kim SW, Han H, Chae GT, Lee SH, Bo S, Yoon JH, et al. Successful stem cell therapy using umbilical cord blood-derived multipotent stem cells for Buerger's disease and ischemic limb disease animal model. Stem Cells 2006;24:1620–6.
[4] Kim SS, Yoo SW, Park TS, Ahn SC, Jeong HS, Kim JW, et al. Neural induction with neurogenin1 increases the therapeutic effects of mesenchymal stem cells in the ischemic brain. Stem Cells 2008;26:2217–28.
[5] Fukuda K, Yuasa S. Stem cells as a source of regenerative cardiomyocytes. Circ Res 2006;98:1002–13.
[6] Pittenger MF, Mackay AM, Beck SC, Jaiswal RK, Douglas R, Mosca JD, et al. Multilineage potential of adult human mesenchymal stem cells. Science 1999;284:143–7.
[7] Yang IH, Kim SH, Kim YH, Sun HJ, Kim SJ, Lee JW. Comparison of phenotypic characterization between "alginate bead" and "pellet" culture systems as chondrogenic differentiation models for human mesenchymal stem cells. Yonsei Med J 2004;45:891–900.

[8] Lisignoli G, Cristino S, Piacentini A, Toneguzzi S, Grassi F, Cavallo C, et al. Cellular and molecular events during chondrogenesis of human mesenchymal stromal cells grown in a three-dimensional hyaluronan based scaffold. Biomaterials 2005;26:5677–86.
[9] Wan C, He Q, McCaigue M, Marsh D, Li G. Nonadherent cell population of human marrow culture is a complementary source of mesenchymal stem cells (MSCs). J Orthop Res 2006;24:21–8.
[10] Gronthos S, Zannettino AC, Hay SJ, Shi S, Graves SE, Kortesidis A, et al. Molecular and cellular characterisation of highly purified stromal stem cells derived from human bone marrow. J Cell Sci 2003;116:1827–35.
[11] Hung SC, Chen NJ, Hsieh SL, Li H, Ma HL, Lo WH. Isolation characterization of size-sieved stem cells from human bone marrow. Stem Cells 2002;20:249–58.
[12] Reyes M, Lund T, Lenvik T, Aguiar D, Koodie L, Verfaillie CM. Purification and ex vivo expansion of postnatal human marrow mesodermal progenitor cells. Blood 2001;98:2615–25.
[13] Jiang Y, Jahagirdar BN, Reinhardt RL, Schwartz RE, Keene CD, Ortiz-Gonzalez XR, et al. Pluripotency of mesenchymal stem cells derived from adult marrow. Nature 2002;418:41–9.
[14] Baddoo M, Hill K, Wilkinson R, Gaupp D, Hughes C, Kopen GC, et al. Characterization of mesenchymal stem cell isolated from murine bone marrow by negative selection. J Cell Biochem 2003;89:1235–49.
[15] Gojo S, Gojo N, Takeda Y, Mori T, Abe H, Kyo S, et al. In vivo cardiovasculogenesis by direct injection of isolated adult mesenchymal stem cells. Exp Cell Res 2003;288:51–9.
[16] Tropel P, Noël D, Platet N, Legrand P, Benabid AL, Berger F. Isolation and characterisation of mesenchymal stem cells from adult mouse bone marrow. Exp Cell Res 2004;295:395–406.
[17] Phinney DG, Hill K, Michelson C, DuTreil M, Hughes C, Humphries S, et al. Biological activities encoded by the murine mesenchymal stem cell transcriptome provide a basis for their developmental potential and broad therapeutic efficacy. Stem Cells 2006;24:186–98.
[18] Li Y, Zhang C, Xiong F, Yu MJ, Peng FL, Shang YC, et al. Comparative study of mesenchymal stem cells from C57BL/10 and mdx mice. BMC Cell Biol 2008;9:24.
[19] Wieczorek G, Steinhoff C, Schulz R, Scheller M, Vingron M, Ropers HH, et al. Gene expression profile of mouse bone marrow stromal cells determined by cDNA microarray analysis. Cell Tissue Res 2003;311:227–37.
[20] Matsuoka S, Ebihara Y, Xu M, Ishii T, Sugiyama D, Yoshino H, et al. CD34 expression on long-term repopulating hematopoietic stem cells changes during developmental stages. Blood 2001;97:419–25.
[21] Mahara A, Yamaoka T. Antibody-immobilized column for quick cell separation based on cell rolling. Biotechnol Prog, in press.
[22] von Andrian UH, Chambers JD, McEvoy LM, Bargatze RF, Arfors KE, Butcher EC. Two-step model of leukocyte-endothelial cell interaction in inflammation: distinct roles for LECAM-1 and the leukocyte beta 2 integrins in vivo. Proc Natl Acad Sci U S A 1991;88:7538–42.
[23] Eniola AO, Willcox PJ, Hammer DA. Interplay between rolling and firm adhesion elucidated with a cell-free system engineered with two distinct receptor-ligand pairs. Biophys J 2003;85:2720–31.
[24] Greenberg AW, Hammer DA. Cell separation mediated by differential rolling adhesion. Biotechnol Bioeng 2001;73:111–24.
[25] Greenberg AW, Brunk DK, Hammer DA. Cell-free rolling mediated by L-selectin and sialyl lewisx reveals the shear threshold effect. Biophys J 2000;79:2391–402.
[26] Hammer DA, Apte SM. Simulation of cell rolling and adhesion on surfaces in shear flow: general results and analysis of selectin-mediated neutrophil adhesion. Biophys J 1992;63:35–57.
[27] Hammer DA, Lauffenburger DA. A dynamical model for receptor-mediated cell adhesion of surfaces. Biophys J 1987;52:475–87.
[28] Fujimoto K, Takebayashi Y, Inoue H, Ikada Y. Ozone-induced graft polymerization onto polymer surface. J Polym Sci A Polym Chem 1993;31:1035–43.
[29] Yamauchi J, Yamaoka A, Ikemoto K, Matsui T. Graft copolymerization of methyl methacrylate onto polypropylene oxidized with ozone. J Polym Sci A Polym Chem 1991;43:1197–203.
[30] Wakitani S, Saito T, Caplan AI. Myogenic cells derived from rat bone marrow mesenchymal stem cells exposed to 5-azacytidine. Muscle Nerve 1995;18:1417–26.
[31] Pittenger MF. Mesenchymal stem cells from adult bone marrow. Methods Mol Biol 2008;449:27.
[32] Meirelles Lda S, Nardi NB. Murine marrow-derived mesenchymal stem cell: isolation, in vitro expansion, and characterization. Br J Haematol 2003;123:702–11.
[33] Komori T, Yagi H, Nomura S, Yamaguchi A, Sasaki K, Deguchi K, et al. Targeted disruption of Cbfa1 results in a complete lack of bone formation owing to maturational arrest of osteoblasts. Cell 1997;89:755–64.
[34] Ducy P, Zhang R, Geoffroy V, Ridall AL, Karsenty G. Osf2/Cbfa1: a transcriptional activator of osteoblast differentiation. Cell 1997;89:747–54.
[35] Otto F, Thornell AP, Crompton T, Denzel A, Gilmour KC, Rosewell IR, et al. Cbfa1, a candidate gene for Cleidocranial dysplasia syndrome, is essential for osteoblast differentiation and bone development. Cell 1987;89:765–71.
[36] Chen JL, Hunt P, McElvain M, Black T, Kaufman S, Choi ES. Osteoblast precursor cells are found in CD34+ cells from human bone marrow. Stem Cells 1987;15:368–77.

///VSP///

Journal of Biomaterials Science 22 (2011) 627–640

Journal of BIOMATERIALS SCIENCE
brill.nl/jbs

Peripheral Nerve Regeneration and Electrophysiological Recovery with CIP-Treated Allogeneic Acellular Nerves

T. Ehashi [a], A. Nishigaito [a,b], T. Fujisato [a,c], Y. Moritan [b] and T. Yamaoka [a,*]

[a] Department of Biomedical Engineering, National Cardiovascular Center Research Institute, 5-7-1 Fujishiro-dai, Suita, Osaka 565-8565, Japan

[b] Department of Medical Engineering, Suzuka University of Medical Science, Suzuka, Japan

[c] Department of Biomedical Engineering, Osaka Institute of Technology, Osaka, Japan

Received 30 October 2009; accepted 19 January 2010

Abstract

Acellular nerve grafts are a desirable alternative to autografts, both because the source of acellular nerves is potentially unlimited and because they have the same matrix structure as natural nerves, which would facilitate axon growth from the defective nerve stump. Although some acellular nerves have been developed, most of them were studied in isogenic transplantation models and evaluated only by histological observation. In the present study, novel allogeneic acellular nerves prepared using the cold isostatic pressuring (CIP) method were developed and assessed as a potential substitute for autografts. The host immune response to acellular nerves and fresh nerves was analyzed using Lewis rats as donors and SD rats as recipients, which is the allogeneic transplantation model, by subcutaneous implantation for one month. In addition, sciatic nerve transplantation into a 10-mm nerve gap was carried out using the same model, and the axonal growth in acellular nerve transplantation was evaluated histologically and electrophysiologically, and compared with that of axons in the autograft transplant area. The subcutaneously implanted acellular nerves contained more macrophages and less vasculature than the allogeneic fresh nerves. In spite of these results of the subcutaneous implantation, Schwann cell infiltration in the graft transplanted into the sciatic nerve gap was observed after the short-term transplantation. The myogenic potential, which was measured as an index of electrophysiological function in acellular nerve transplantation, was also recovered in the long-term transplantation. Our results indicate that the acellular nerves developed herein have the potential to support nerve regeneration and might be useful as an alternative to autografts.

Keywords

Acellular nerve, allogeneic, electrophysiological study, cold isostatic pressuring treatment

1. Introduction

Autologous fresh nerves are commonly used in clinical applications for treating peripheral nerve defects. However, an alternative to the autologous nerves is needed because these nerves are available only in limited quantities, and also because their use causes concurrent healthy nerve dysfunction [1, 2]. In general, tissue-derived nerves are always preferable, since they possess a natural internal structure of extracellular matrix components, which can lead to cellular migration and nerve fiber elongation [3–7].

Cadaveric donor grafts are an attractive alternative to autologous nerves, and their supply is potentially unlimited. In 2001, clinical trials for cold-preserved nerve allografts were reported to cause severe peripheral nerve defects [8]. In that report, 6 patients exhibited successful nerve reconstruction by cadaveric nerve allograft transplantation. However, long-term systematic administration of immunosuppressant was required, and even with that degree of treatment, one of the patients still experienced immune rejection. Moreover, it has been reported that the rate of nerve regeneration using cold preserved allogeneic nerves is lower than that using autologous fresh nerves with immunosuppressant treatment [9].

For treatment without an immunosuppressant, various strategies to eliminate the immunogenicity of allogeneic nerves have been explored in different animal models, but the grafts revealed very poor completeness in comparison to that of the autografts [10–12]. The main strategies for reducing the immunogenecity of allografts or xenografts are thermal and chemical pretreatments of nerves [8, 13, 14]. These pretreatments can destroy or remove the donor cells, but the natural internal structure of the nerve tissue remains unchanged.

The thermal process involves repeated cycles of freezing and thawing of donor nerves. This process destroys the allogeneic antigen and eliminates allogeneic cells, and has been reported to decrease the host antigeneic response in some studies [8, 15]. However, the axonal growth in these grafts is slower than it is in fresh autografts or isogeneic grafts, because of the residual allogeneic cells in the graft [13]. The cellular debris in the graft leads to macrophage invasion and basal laminae damage, which delay the nerve regeneration [16–19].

Chemical processes to remove the donor cells with detergents have been studied not only for peripheral nerve tissue [14, 20, 21] but also for cardiac muscle [22], heart valves [23] and pericardium [24]. This process is more effective in removing the donor cells. However, it also causes more damage to the extracellular matrices than thermal pretreatment does [7, 25, 26]. In addition, it is difficult to completely remove the detergent from the graft, and the residual chemicals suppress tissue regeneration. Starting in 2002, decellularized human nerves which are processed with a combination of detergent decellularization, chondroitinase degradation and gamma-irradiation sterilization have been marketed by AxoGen in the USA. The decellularized nerve grafts are superior to the commercially available conduits but not as effective as isografts [27].

We have established a novel decellularization method using a cold isostatic pressuring (CIP) treatment [28]. This method has succeeded in removing the cellular components from pig blood vessels, heart valves and trachea. We have also reported on the excellent reconstruction of endothelial cells, fibroblasts and smooth muscle cells in acellular vessels 12 weeks after the transplantation [28]. Thus, novel allogeneic acellular nerve grafts that possess natural extracellular matrices were prepared by the CIP method and examined in this study. In fact, many studies have been performed to develop novel treatments as an alternative to autografts, and most of the acellular tissue transplantations have been studied using isogeneic transplantation models [2, 20, 29, 30]. However, only a few studies have focused on allogeneic transplantation [8, 21, 26, 31]. Moreover, the regeneration of nerves by pretreated nerve transplantation should be assessed functionally in addition to histological assessment. For example, there have been only a few studies focused on the conduction velocity [20, 32] or myogenic potential [20, 31] of the acellular nerve transplantation. Therefore, for this study, allogeneic acellular nerves were prepared from Lewis rat sciatic nerves, and transplanted into a sciatic nerve gap in SD rats. As a preliminary study, a 10-mm gap of sciatic nerve which is repaired by any other nerve graft substitute, was bridged with our acellular nerve grafts to evaluate their potential in nerve regeneration, and the axonal growth in the allogeneic acellular nerves was evaluated histologically and electrophysiologically.

2. Materials and Methods

2.1. Preparation of Acellular Nerves

All animal studies were performed in accordance with the guidelines of the Ministry of Health, Labour and Welfare of Japan, as well as the guidelines of our institution, and approved by the Institutional Animal Care and Use Committee at the National Cardiovascular Center Research Institute.

Approximately 30-mm lengths of the sciatic nerves were harvested from a male Lewis rat weighing 300–350 g (Japan SLC) and, after trimming their peripheral fat and connective tissues, the nerves were packed in a polyethylene pouch with Ca^{2+}-, Mg^{2+}-free phosphate-buffered saline (PBS; Invitrogen) and the air was expelled. The nerves were then treated with ultra high pressure of 980 MPa at 30°C for 10 min using a Dr. Chef high pressure food processor (Kobe Steel) to disrupt all cells, microorganisms and viruses inside the tissues. The cell debris was washed away by immersing the cells in endothelial cell growth medium (EGM-2 Bulletkit; Lonza) for 2 weeks at 37°C. Then, ethanol/PBS (80:20, v/v) was used to remove phospholipids, which lead to calcification of implants, and was removed by rinsing with PBS for 3 days.

The acellular nerves were morphologically and histologically compared with the untreated nerves. The decellularization efficiency and extra-cellular component morphology were evaluated by hematoxylin and eosin staining (HE staining). Briefly, the samples were fixed with 10% neutralized formalin, then dehydrated and

embedded in paraffin, sectioned at 8–10 μm, and captured on slide glasses. The slide glasses were immersed into Mayer's hematoxylin solution (Wako), rinsed with tap water, and counterstained with eosin solution (Wako).

2.2. Subcutaneous Implantation

The host body reaction to the allogeneic fresh nerves and allogeneic acellular nerves was investigated by subcutaneous implantation into rats. As the allogeneic transplantation model, we used Lewis rats and SD rats as donor and recipient animals, as described by Hudson *et al.* [17]. Three 13-week-old male SD rats (Japan SLC) were anesthetized with isoflurane inhalation. Two incisions were made in the dorsal skin on the back of each of three SD rats, and fresh or acellular nerves of a Lewis rat (10 mm long) were inserted into both subcutaneous spaces. Thus, one fresh nerve sample and one acellular nerve sample was implanted into the back of each of the three rats. After 4 weeks of implantation, all rats were killed humanely and the grafts were resected with the surrounding skin.

Angiogenesis and macrophage infiltration against the grafts was evaluated by HE staining ($n = 3$) and immunostaining for von Willebrand Factor (vWF) ($n = 1$) and CD68 ($n = 3$). All resected tissues with graft were fixed with 10% formalin, dehydrated with gradient alcohol and embedded in paraffin. All nerves were sectioned at 4 μm thickness and the middle parts of the grafts were used for staining. For the primary antibody, anti-vWF antibody (Dako) and anti-CD68 antibody (AbD Serotec) were used, and horseradish peroxidase-conjugated secondary antibody (Dako), 3,3-diaminobenzidine substrate (Dako) and eosin solution (Wako) were used to visualize the cells.

The total numbers of infiltrated cells and macrophages in implants and the number of blood vessels with a luminal structure were calculated. The total numbers of cells and macrophages were analyzed using free imaging soft, ImageJ (NIH). Pictures were taken at 40× magnification, and the numbers of nuclei and stained cells were counted using particle analysis tools included in the software package. In HE staining and immunostaining for CD68, three areas were randomly selected within implanted nerves. Blood vessels with a circular form with vWF positive cells inside the grafts were counted visually.

2.3. Implantation of Graft in the Sciatic Nerve Defect

The allogeneic acellular nerves prepared by CIP treatment were transplanted to rat sciatic nerve defect models. The recipient animals, 6 SD rats, were anesthetized by isoflurane, and both sides of the sciatic nerves were exposed. A 10-mm length of the right-side sciatic nerve was excised, and an acellular nerve graft of the same length was sutured at both stumps of the recipient nerve using 10-0 vicryl (Ethicon) under a microscope. Another side sciatic nerve was excised, and the excised nerve was reversed and sutured in the same way as the autograft control. Four of the transplanted animals underwent electrophysiological and histological study, and the others were only used for histological evaluation.

2.4. Assessment of the Transplanted Nerves

The transplanted grafts were electrophysiologically evaluated by electromyograms in the short-term (158 days; $n = 1$) and long-term (247, 248 and 258 days; $n = 1$ each) experiments. Under anesthesia, both sides of the sciatic nerves were exposed from the proximal to the distal parts of the graft positions. The proximal part of the nerve was hooked with two platinum wire electrodes and stimulated with 1 V monophagic rectangular voltage with 10 μs duration at a frequency of 1 Hz (Nihon Koden). The myogenic potential of the tibial muscle group was recorded by inserting two needle-type electrodes, amplified (Nihon Koden) and acquired by a PowerLab system (AD Instruments). In all cases, 50 traces were recorded and averaged.

In the histological evaluation, sciatic nerves including the graft were resected at 110 days ($n = 1$) and 158 days ($n = 1$) post-operation. The nerves were fixed with 10% neutralized formalin, dehydrated and embedded in paraffin. Then, the tissues were sliced longitudinally in sections of 4 μm thickness each, and the middle parts of the grafts were stained using HE or anti-glial fibrillary acidic protein (GFAP) antibody (Dako), which stains Schwann cells in peripheral nerves. The anti-GFAP was visualized with labeled polymer (Dako) according to the manufacturer's specifications. Hematoxylin staining (Wako) was carried out as a counterstaining measure to visualize the nuclei.

2.5. Statistical Analysis

The total number of cells and macrophages in the subcutaneous implantation experiments was counted. The mean values of all parameters were determined along with their standard deviations. Student's t-tests were applied to determine the statistical significance of differences between numbers of total cells and macrophages in allogeneic fresh or allogeneic acellular grafts. Values of $P < 0.05$ were considered to indicate statistical significance.

3. Results

3.1. Decellularization of Rat Sciatic Nerves

Acellular rat sciatic nerves were prepared by destroying cells using CIP treatment and a washing process. At two time points, i.e., immediately after CIP treatment or after CIP treatment plus 3 weeks of washing, nerves were histologically compared with untreated fresh nerves by hematoxylin and eosin (HE) staining and immunostaining for GFAP (Figs 1 and 2). The results showed that CIP treatment alone could not remove the cells (Fig. 1B). After the washing process, all cells were removed from the tissue, and fiber-like extracellular matrices (ECM) were left behind (Fig. 1C). On the other hand, there were many nuclei present among the dense matrices in the untreated fresh nerves (Fig. 1A). Immunostaining showed that the Schwann cells in the nerves completely disappeared after decellularization (Fig. 2B). These histological observations showed that the decellularization process

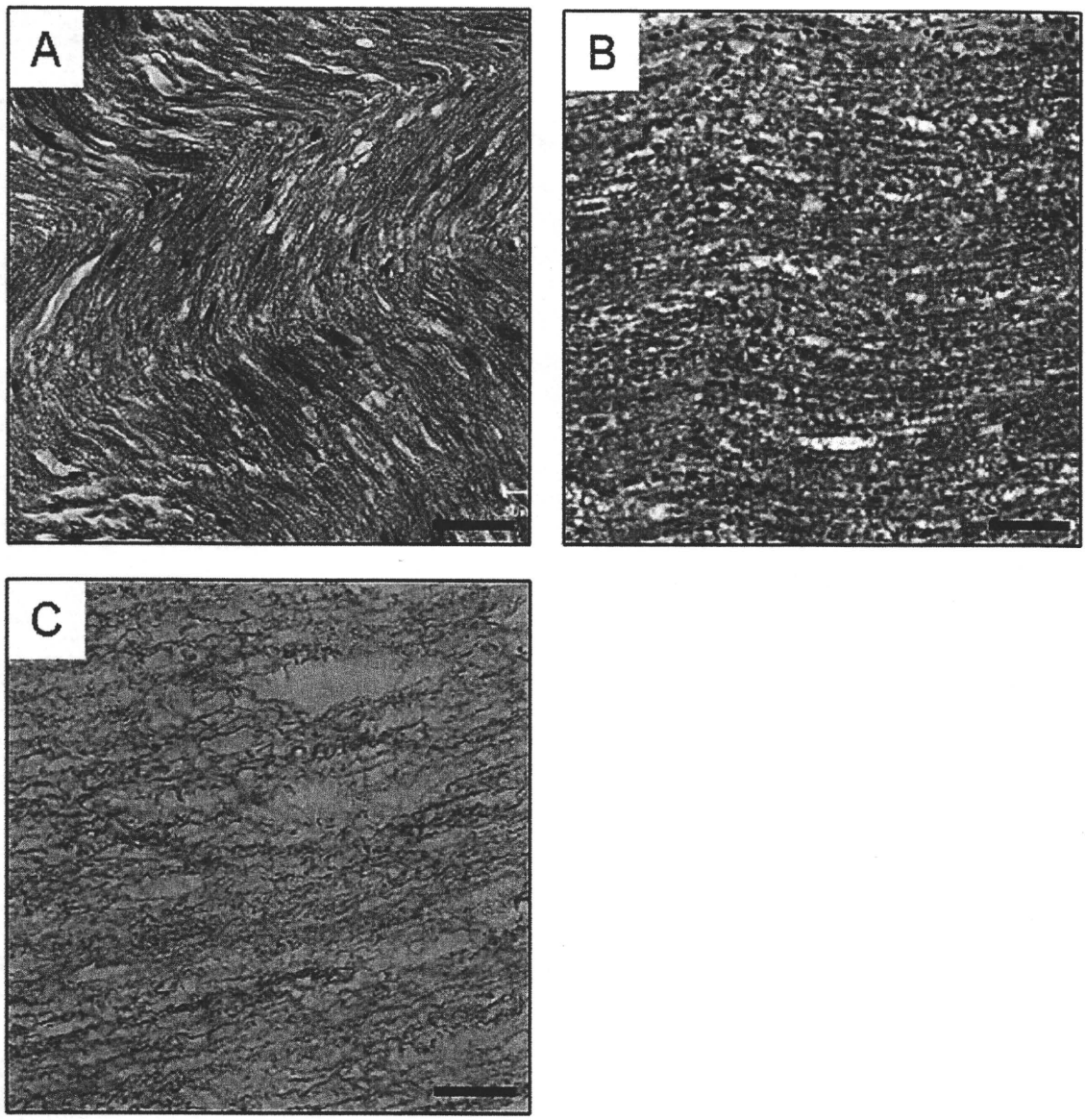

Figure 1. HE staining of a fresh nerve (A), a nerve just after CIP treatment (B) and a nerve after the complete washing process (C). Scale bars = 50 μm.

succeeded in the removal of cellular components while retaining the nerve ECM. The remaining ECM maintained an intrinsic orientation that is expected to be effective for axonal growth.

3.2. Host Body Reactions to Allogeneic Fresh and Acellular Nerves

To investigate how the decellularization process affects the host body reaction, fresh and acellular nerves of Lewis rats were implanted subcutaneously into the SD rats and assessed histologically. At 1 month post-operation, many cells had infiltrated in both grafts (Fig. 3). However, the cell shapes were quite different between the fresh nerve and the acellular nerve. Many cells in the fresh nerve showed spindle-shaped nuclei and cytoplasms, whereas round shapes were seen in the acellular nerve (Fig. 3A and 3B). Immunostaining for CD68 showed that most cells in the

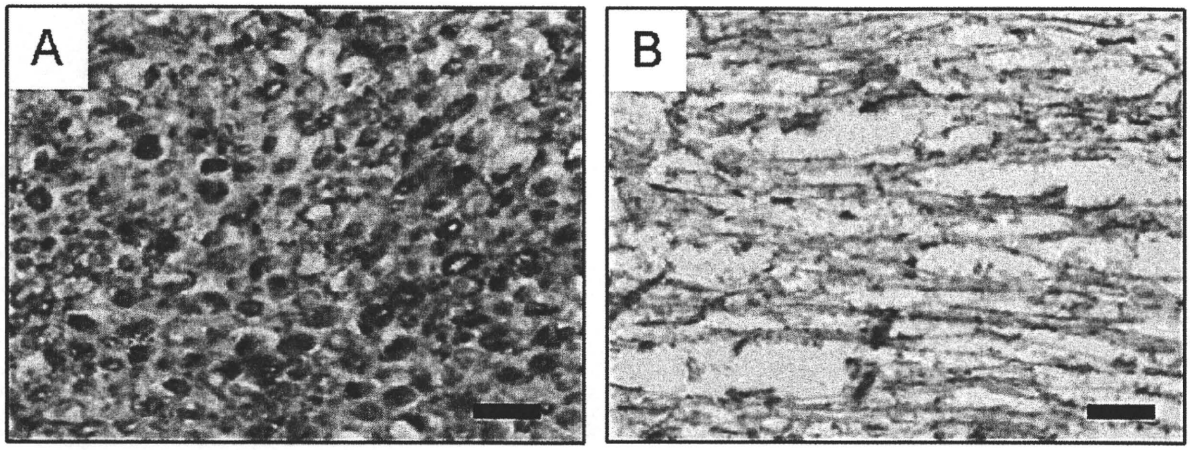

Figure 2. Immunostaining for GFAP of fresh (A) and acellular (B) nerves before implantation. Scale bars = 50 μm.

acellular nerves were macrophages while there were very few CD68-positive cells in the fresh nerves (Fig. 3C and 3D). The total numbers of cells and CD68-positive cells are summarized in Fig. 4. The total cell densities in the fresh and acellular nerves were the same. However, most cells in the acellular nerves were CD68-positive cells, whereas there were almost no CD68-positive cells in the fresh nerves. The major cell population in the fresh nerves could not be identified from immunostaining.

Angiogenesis in the graft was visualized by vWF immunostaining (Fig. 3E and 3F). When the fresh nerve was implanted, many small capillaries were present inside the graft (495 capillaries), and the surrounding subcutaneous tissue had normal vessels. On the other hand, when the acellular nerve was implanted, angiogenesis did not occur in the graft (19 capillaries), but blood vessels with a larger diameter did appear in the surrounding tissues. These observations suggest that the decellularization process might have changed the characteristics of the nerves and caused a different host body reaction in comparison to that elicited by the fresh nerves.

3.3. Histological Evaluation of the Acellular Nerve Grafts

Histological evaluation of the transplanted grafts was carried out by HE staining and immunostaining for GFAP on 110 days and 158 days after the operation (Fig. 5). Both in the fresh autograft and in the acellular allogeneic graft, remarkable cellular infiltration was observed by HE staining, even at 110 days after transplantation. Most of these cells were aligned in the longitudinal direction of the nerves, but rarely formed a fiber-like morphology at that point on time. On the other hand, 158 days after transplantation, many fibrous structures in the long-term transplantation were observed, especially in the autologous fresh nerve.

Immunostaining for GFAP in the Schwann cells in the peripheral nerves showed that the Schwann cells had infiltrated the host nerves. At 110 days post-operation,

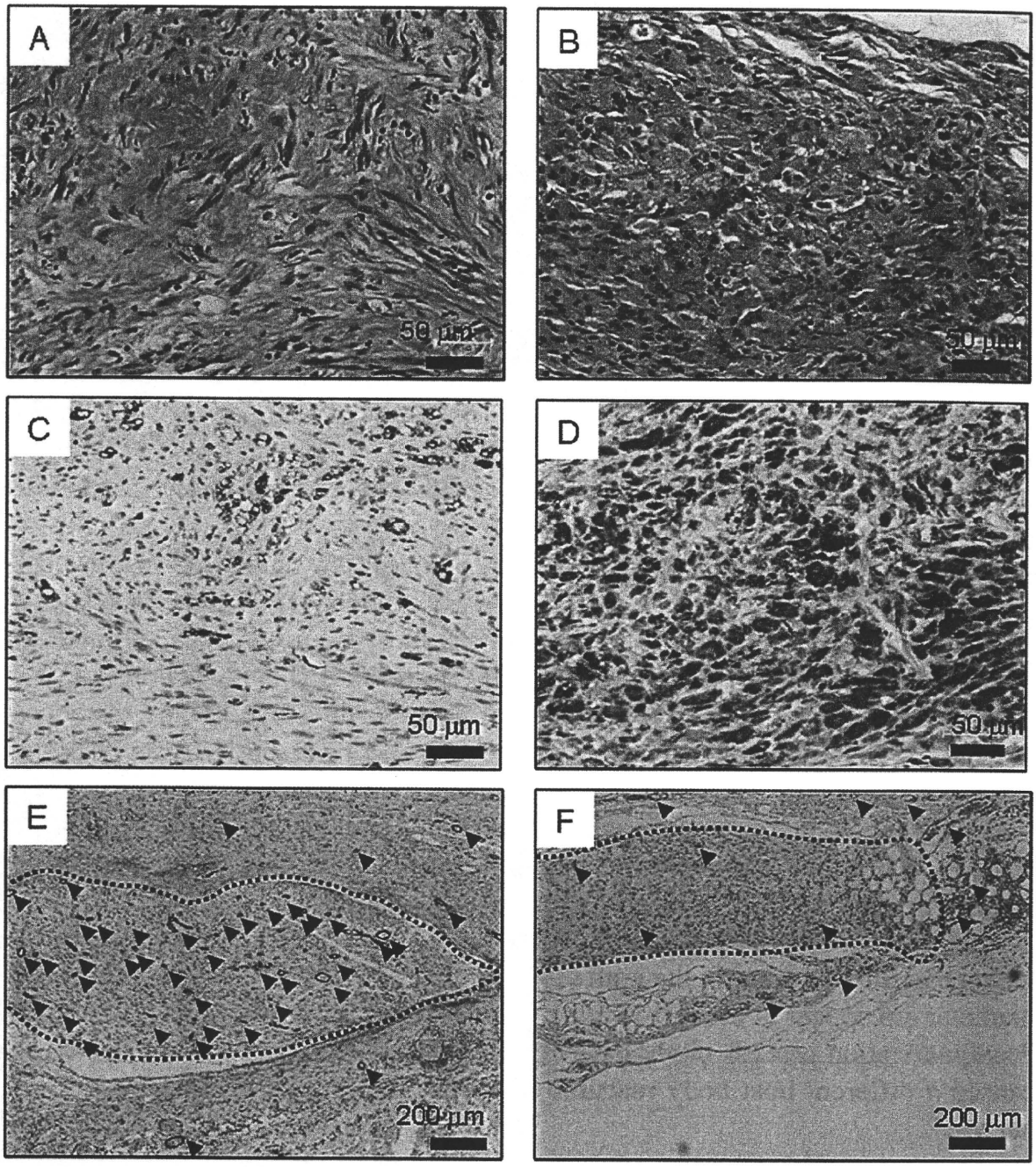

Figure 3. HE staining (A, B) and immunostaining for CD68 (C, D) and vWF (E, F) in subcutaneously implanted allogeneic fresh (A, C, E) and allogeneic acellular (B, D, F) nerves 1 month postimplantation. The images of HE staining and immunostaining for CD68 show the middle areas of the implant. The dotted lines and arrowheads in E and F indicate the edge of the grafts and microvessels, respectively. This figure is published in colour in the online edition of this journal, that can be accessed *via* http://www.brill.nl/jbs

a few GFAP-positive cells with fiber-like morphologies were observed in autologous fresh nerves but not in the allogeneic acellular graft. At 158 days after the time of transplantation, both grafts showed a fiber-like formation of GFAP-positive cells. At that time point, the acellular grafts included cells with thinner fiber-like morphology than the fresh nerves.